Determination of pore fractal dimensions and porosity of silica glasses from the dielectric response at percolation

Alexander Puzenko, Nick Kozlovich, Anna Gutina, and Yuri Feldman*
Department of Applied Physics, The Hebrew University of Jerusalem, 91904, Jerusalem, Israel
(Received 26 February 1999; revised manuscript received 9 June 1999)

The analysis of the dielectric relaxation spectrum at percolation was used for the determination of the dimensions of pore fractals and porosity of silica glasses. The percolation phenomenon in the porous glasses is related to the transfer of the electric excitation within the developed network of open pores due to migration of protons and ions along the pore surface of connected pores. The dielectric spectroscopy technique allows us to identify the relaxation process related to percolation, and to extract the fractal dimensions of the paths of excitation transfer associated with migration of charge carriers within the porous medium. The random fractal model describes the geometrical disorder of the porous matrix. In the framework of this model, the relationship between the porous space fractal dimension and the porosity of the medium has been obtained. The juxtaposition of the structural and the relaxation models enables us to derive the relationship between the value of porosity and the fractal dimensions of the paths of excitation transfer within the porous medium. The experimental porosity values for several porous silica glasses obtained by means of the developed theoretical approach and dielectric spectroscopy measurements are presented. The porosity values obtained from the dielectric spectroscopy method are found to be in good agreement with the data obtained from the measurements of the relative mass decrements. [S0163-1829(99)11743-0]

I. INTRODUCTION

Recently, much attention has been paid to porous silica glasses obtained from sodium borosilicate glasses. The irregular structure and the morphology of the involved porous medium are a matter of interest in many industrial processes.[1–3] For instance, the moisture-holding capacity, transport phenomena, and dynamics of molecules of liquids and solids confined in the pores are all related to the pore geometry.

A silica porous glass can be defined as a bicontinuos random structure of two interpenetrating percolating phases, namely the solid and the pore networks. The pores in the glasses are connected to each other and the pore size distribution is narrow. The characteristic pore spacing depends on the method of preparation, and can be between 2 and 500 nm. The bicontinuos structure is obtained as a result of spinodal decomposition of the two phases SiO_2 and $B_2O_3+Na_2O$ and formation of the interfacial layer during the formation process. This layer can be destroyed after leaching out the acid-soluble phase $B_2O_3+Na_2O$ with formation of the developed porous morphology and large surface to volume ratio. A typical example of silica glasses is Vycor glass. The properties and morphological characteristics of Vycor glass have been studied extensively due to the features of this glass has in common with porous materials of technological interest.

In order to augment our understanding of the effect of the structure on the properties of the silica glasses, the first step and challenge is to characterize the morphology of such materials and, in particular, such parameters as pore and surface *fractal dimensions* as well as their *porosity*. The fractal dimensions of solids are determined mainly by small angle x-ray and neutron scattering (SAXS and SANS),[4–16] microscopy,[17,18] electronic energy transfer techniques,[19–23] etc. The molecular probe method and its modifications using adsorption can also play an important role in the determination of the fractal dimensions of a porous medium.[24–29]

There are numerous contradictions and discussions in the literature regarding both the *volume and surface fractal structures* in Vycor glasses.[12–14,20,21,23,25,30,31] A significant chemical interaction between the adsorbed water and the pore surface with the possible formation of a gel-like state can significantly modify the surface morphology of the pores in silica porous glasses. Most of the information related to the pore morphology was obtained from transmission electron microscopy, adsorption techniques, and small-angle-scattering techniques.[12–14,21,22,25,30–36] For example, an analysis of the small-angle scattering pattern from dry Vycor suggest that the glass possesses a rough surface with a fractal dimension of $D\sim 2.5$, and with the upper length cutoff <20 Å (Ref. 14). However, several other investigations show no evidence of surface fractality in H_2O-saturated samples.[12,37] In recent investigations[6,13,31,35] it has been shown that a fractal surface can defractalize upon deposition of an adsorbed film of water. Particularly, a small amount of water, 3% w/w, is sufficient to render the surface smooth. Regarding the fractality of the pore volumes, the question is hitherto even more puzzling. On the one hand, the energy-transfer measurements suggest that the pore structure of Vycor glass is fractal on the length scale <100 Å with a fractal dimension of 1.74 ± 0.12 (Refs. 21 and 38). This rather small value of D was imputed to a three-dimensional percolation cluster backbone without dangling bonds.[38] On the other hand, a fractal geometry was indicated in Vycor glass on a length scale larger than 1000 Å with the percolation network formed by the empty pores and the value of fractal dimension of 1.7 (Refs. 6 and 30). This value concurs well with the data obtained from the energy-transfer measurements. Con-

trary to that result, it was noted[14] that the SANS, and SAXS data leave little room for the idea that Vycor glass has a fractal pore network on a scale above 40 Å.

For characterization of *porosity* in glasses, the most successful and popular techniques are image analysis, scattering techniques, adsorption techniques, and mercury porometry.[4,12,20,24,25,30,39–47] The most significant drawback of the traditional methods of porosity determination is that they are not always accurate regarding the length scales involved in the measurement. Indeed, it is important to bear in mind that each of the above-mentioned techniques has its own range of applicability depending on the sizes of the pores.[48] In particular, gas-adsorption methods are sensitive to micro- and mesopores on a length scale of 10^{-10}-10^{-7} m (Ref. 41), scattering methods SAXS and SANS allow one to study the mesoscale range of pore sizes of 10^{-9}-10^{-7} m (Refs. 4, 12, and 30), and the mercury porosimetry method is appropriate for the macroscopic scales of 10^{-5}-10^{-7} m (Ref. 40). Therefore, both the porosity values for the fractal medium and the aforementioned fractal dimension depend on the scale for which the measuring technique is appropriate.[49]

In addition to the techniques mentioned above, the NMR and dielectric relaxation properties of porous media are also found to be very sensitive to the geometrical micro and mesostructural features of the porous matrix.[48,50] The dielectric spectroscopy can be applied when the pore space is filled with a conductive or nonconductive dielectric material. The response also depends on the properties of the materials filling the pores.[51–56] The determination of porosity from dielectric spectroscopy is mainly based on the mixture formulas.[55–60] Recently a theoretical framework, based on a geometric characterization of porous media whose the pore space is filled with a conductor, introducing the local porosity distribution and local probabilities has been proposed.[48,61,62] This local porosity theory is based on the effective medium approximation and percolation scaling model employed for the matrix-filler two-phase medium. An application of these approaches to the determination of porosity requires a filling of the whole pore space with a conductor or dielectric material in order to make the matrix-pore media a two-phase system. However, the filling the entire pore space can be only performed in the case of connected pores. Meanwhile, even in the percolating porous space, if the pore surface has a fractal nature, then it is an impossible task to fill up all the voids.

One alternative to the aforementioned approach for inferring the morphology of porous glasses is a method based on the analysis of the dynamics of water molecules that can easily be absorbed from ambient air. Indeed, as it has been shown in Ref. 35 even ''dry'' silica glasses can contain three types of adsorbed water on the pore surface. The first type forms a physisorbed layer, which is desorbed by heating at 90 °C. The second and third types form a chemisorbed layer associated with spatially distributed individual molecules (or groups of several molecules) on the surface. The second type of water comes off above 190 °C, while the third type is a more strongly chemisorbed layer, consisting of water clusters of 40–60 molecules,[35] connected to each other by hydrogen bonds and forming an ordered array of water molecules. The dynamic properties of adsorbed water are different from those of bulk water.[63] The dielectric spectroscopy method based on the analysis of the dynamics of water does not require the above-mentioned water saturation experiments and deals only with a thin layer of water molecules adsorbed from the atmosphere.

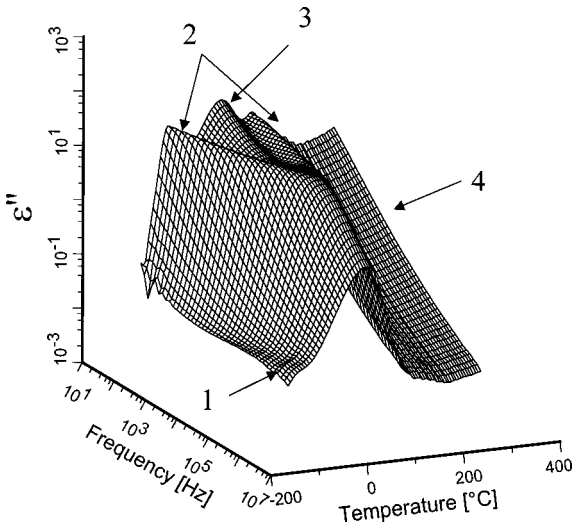

FIG. 1. Three-dimensional plot of the frequency and temperature dependence of the dielectric losses of sample 2 (see Sec. III).

In our prior paper,[64] we investigated the dielectric properties associated with the relaxation of water molecules in the adsorption layer of several silica glasses over broad regions of frequency and temperature with the purpose of studying the dynamics and inferring the morphological properties of the porous materials. It was shown that the complex dielectric behavior could be described in terms of the four distributed relaxation processes. The typical spectrum of the dielectric losses associated with the relaxation of water molecules from the adsorptive layer for the studied porous glasses versus frequency and temperature is displayed in Fig. 1. The first relaxation process which is observed in the low temperature region -100 °C to $+10$ °C is due to the reorientation of water molecules in icelike structures of water clusters. The second relaxation process has a specific saddlelike shape and is well marked in the temperature range -50 to $+150$ °C. This relaxation process is thought to be a kinetic transition due to the water molecule reorientation in the vicinity of defects. The third process is located in the low-frequency region and the temperature interval 50–80 °C. This process shows several specific features. Thus, the amplitude of this process essentially decreases when the frequency increases. Further, the maximum of dielectric losses has almost no temperature dependence. At last, when the temperature approaches to the magnitude related to the third relaxation process, electric conductivity significantly increases (Fig. 2). As shown in the literature,[65] these aforementioned features indicate that this process is related to percolation. Indeed, the percolation associated with the proton transport in silica glasses is known in the literature[65,66] in the temperature range of the third process. Therefore, we associate the third relaxation process with the percolation of an electric excitation within the developed fractal structure of connected pores due to migration of the protons and ions filling the porous space.

In the high-temperature region, above 150 °C, the glasses show an increase in dielectric constant and dielectric losses

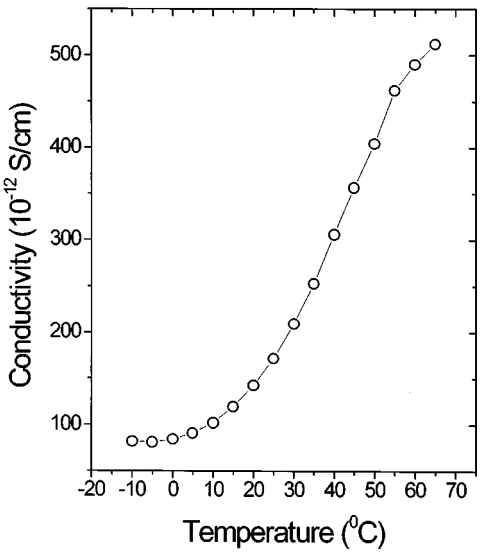

FIG. 2. Temperature dependence of the low-frequency conductivity of sample 2 (see Sec. III).

in the low-frequency limit. This relaxation process is thought to be related to the Maxwell-Wagner-Sillars polarization process as a result of the trapping of free charge carriers at the interface, thus causing a build up of macroscopic charge separation, or space charge with a relatively long-relaxation time.

The aim of this paper is to further analyze the complex relaxation behavior of the third relaxation process, which is associated with transfer of the electric excitation at percolation, with the purpose of inferring the geometrical features of the porous silica glasses from its dielectric response. In this paper, we will use the idea of the method of electronic energy transfer dynamics developed by Klafter, Blumen, and Shlesinger[67,68] and further employed by several authors[21,22,38] in order to determine the fractality of the porous silica glasses. The idea will be used for the description of the electric excitation at percolation within the developed fractal structure of the porous glasses. Note that in the silica porous glasses the excitation transfer is associated with the migration of ions and/or protons along the pore surface of connected pores.[65,66,69] We shall further develop a statistical fractal model, which establishes a relationship between the fractality of the porous space and porosity of the material. The approach developed will be applied to the investigation of porous glasses with controlled morphological parameters. The dimensions of pore fractals and porosity of silica glasses corresponding to the macroscopic length scale will be determined from dielectric spectroscopy study and compared with the data obtained from measurements of the relative mass decrements.

II. THEORETICAL BACKGROUND

A. Description of a porous medium in terms of regular and random fractals

1. Porosity in the regular fractal model

Porous materials are complex systems with a big inner surface of boundaries between different phases of compound substances. The fundamental numerical characteristic of a porous matrix is the macroscopic porosity. The porosity ϕ of a two-phase solid-pore system can be defined as the ratio of the mean volume of the whole empty space volume V_p, to the whole volume V, of a sample

$$\phi = \frac{V_p}{V}. \tag{1}$$

Disordered porous media have been adequately described by a fractal concept.[70–72] As we mentioned in the introduction, many real porous materials show fractal structures on some pore space length scales. The solid-pore interface can also be fractal. By assuming that the volume of pore space is determined by the fractal structure, the *regular fractal model* can be applied. This implies that for a volume element of linear macroscopic size H, the volume of pore space is given in units of the characteristic pore size h by $V_p = G(H/h)^D$, where D is the regular fractal dimension of the system, H coincides with the upper and h with the lower limit of the self similarity. The constant G is a geometric factor. By the same token, the volume of the whole sample is scaled in units of h as $V = G(H/h)^d$, where d is the Euclidean dimension ($d=3$). Hence, the formula for the porosity in terms of the regular fractal model can be derived from Eq. (1), and it is given by

$$\phi = \left(\frac{h}{H}\right)^{d-D}, \tag{2}$$

Equation (2) has been used for the analysis of the fractal sandstone pores.[17] It was also applied for porosity estimations in porous Vycor glass.[49] We note that the agreement between the value of the porosity obtained from various experimental techniques and the value of porosity determined from Eq. (2) will be only in the case when the three following conditions are fulfilled. Firstly, the scale interval of the measuring technique must coincide with the interval of self similarity of the porous medium. Secondly, the fractal dimension in the measuring interval must be a constant value. Thirdly, the value of the ratio h/H is a determined value for a selected measured sample. In this case, the parameter ϕ in Eq. (2) has a meaning of the macroscopic porosity of a material.

2. Porosity in the random fractal model

In general, real porous systems and measuring intervals used in different techniques do not comply with the three conditions mentioned above and the regular fractal model is not valid. In order to embrace variety of porous media and experimental techniques when these conditions are not fulfilled, the *random fractal* models can be considered.[70] This model enables us to take into account the dependence of measuring porosity of a medium on the scale of observation. Randomness can be introduced in the regular fractal model of porous medium by one or both of the following: we can assume that (i) the fractal dimension of the structure is random; and/or (ii) the scale parameter, which is equal to the ratio $\xi = h/H$ of the lower and upper cutoffs of the self-similarity range is a random value. Further, we assume that parameter ξ is distributed in the interval $[\lambda/\Lambda, 1]$, where λ

TABLE I. The several known distribution laws derived from the general exponential distribution function $w(\xi)=A\xi^{\alpha}\exp(-b\xi^{\beta})$ at various values of the parameters.

N^0	Values of the parameters	Region of changes of the function argument	Type of distribution
1	$\alpha<0,\ b=0$	$\mu\leqslant\xi\leqslant 1$	Power
2	$\alpha=0,\ b>0,\ \beta=2$	$-\infty\leqslant\xi\leqslant\infty$	Normal
3	$\alpha=1,\ b>0,\ \beta=2$	$0\leqslant\xi\leqslant\infty$	Reyleigh
4	$\alpha=1,2,3...,\ b>0,\ \beta=1$	$0\leqslant\xi\leqslant\infty$	Poisson
5	$-1\leqslant\alpha\leqslant\infty,\ b>0,\ \beta=1$	$0\leqslant\xi\leqslant\infty$	Gamma
6	$\alpha=u/2-1,\ b=1/2,\ \beta=1,$ where u is the number of the degrees of freedom	$0\leqslant\xi\leqslant\infty$	χ^2
7	$\alpha=0,\ b>0,\ \beta=1$	$0\leqslant\xi\leqslant\infty$	Exponential
8	$\alpha=3,\ b>0,\ \beta=1$	$0\leqslant\xi\leqslant\infty$	Plank
9	$\alpha=0,\ b>0,\ \beta=0$	$\mu\leqslant\xi\leqslant 1$	Uniform
10	$\alpha<0,\ b>0,\ \beta>0$	$\mu\leqslant\xi\leqslant 1$	Percolation

and Λ are the minimal and maximal boarders of the measuring interval $[\lambda,\ \Lambda]$. If the whole volume is divided into macroscopic cells of the linear size Λ (for organization of a statistical ensemble), then the probability for a given cell to find some scale parameter and fractal dimension within the rectangle from ξ to $\xi+d\xi$ and from D to $D+dD$ is $W(\xi,D)d\xi dD$. The bulk porosity can be considered as the integral over statistical ensemble of the cells and is determined by

$$\Phi\equiv\langle\phi\rangle=\int_{\Omega}\int\phi(\xi,D)W(\xi,D)d\xi dD, \tag{3}$$

where the angular brackets denote an ensemble average and Ω is the boundary region of the possible changes of ξ and D. In the first limiting case, when the fractal dimension is random but the scale parameter is a constant independent of D, Eq. (3) is equivalent to a multifractal model of a medium.[73,74] In the second limiting case,[70] when the scale parameter is random in the interval $[\lambda/\Lambda,\ 1]$, but the fractal dimension in this interval is a determined constant, Eq. (3) reads as

$$\Phi=\int_{\mu}^{1}\phi(\xi,D)w(\xi)d\xi, \tag{4}$$

where $\mu=\lambda/\Lambda$ is the minimal value of the scale parameter ξ on the interval $[\lambda/\Lambda,\ 1]$, and $w(\xi)$ measures the probability density to find some scale parameter in the range from ξ to $\xi+d\xi$, and it is related to the distribution function of the spatial scales on the interval $[\lambda,\ \Lambda]$.

The measuring techniques mentioned in the introduction provide a value of the fractal dimension on a certain scale interval. Therefore, in this paper, for calculation of the porosity of a fractal medium we will be focused on the second statistical approach, wherein the assumption of the unchanged fractal dimension on the interval $[\lambda/\Lambda,\ 1]$ is considered and the effect of pore-size polydispersity is taken into account.

In the current approach, we permit the analytical equations, which describe the pore-size distributions of various porous media, or even in one porous material considered on the different scales, to be different. In order to take into account this variety we use a generalized exponential distribution function for the parameter ξ. This distribution includes most of the known distribution functions used in the literature.[75–77] In this case the probability density can be written as

$$w(\xi)=A\xi^{\alpha}\exp(-b\xi^{\beta}), \tag{5}$$

where the normalization constant A is determined from the normalization condition $\int_{\mu}^{1}w(\xi)d\xi=1$, and it reads as

$$A=\left[\int_{\mu}^{1}\xi^{\alpha}\exp(-b\xi^{\beta})d\xi\right]^{-1}. \tag{6}$$

The distribution function of Eq. (5) includes three empirical parameters, α, β, and b. Table I summarizes various known distribution laws derived from the general exponential distribution function [Eq. (5)] at various values of the parameters. The parameter b is related to the effective cutoff length, ξ_{eff}, as $b\sim(\xi_{\mathrm{eff}})^{-\beta}$. The physical meanings of the parameters α and β can be assigned after ascertaining the relationships between these parameters and the properties of fractal morphology and polydispersity of the finite-pore size.

By substituting Eqs. (2) and (5) into Eq. (4) and using Eq. (6), we obtain the relationship for the mean macroscopic porosity as

$$\Phi=\frac{1}{b^{(d-D)/\beta}}\times\frac{\Gamma\left(\frac{1+\alpha+d-D}{\beta},b\mu^{\beta}\right)-\Gamma\left(\frac{1+\alpha+d-D}{\beta},b\right)}{\Gamma\left(\frac{1+\alpha}{\beta},b\mu^{\beta}\right)-\Gamma\left(\frac{1+\alpha}{\beta},b\right)}, \tag{7}$$

where $\Gamma(q,x)=\int_{x}^{\infty}\xi^{q-1}\exp(-\xi)d\xi$ is the incomplete Gamma function.

The stretched exponential cutoff factor, $\exp(-b\xi^{\beta})$, in Eq. (5) characterizes an effective cutoff of the length scale distribution function. With increasing ξ from the range where

$\xi < \xi_{\text{eff}}$ to range where $\xi > \xi_{\text{eff}}$, this factor describes a transition from the scaling regime, characterizing a mesoscale range, in which $w(\xi) \sim \xi^{\alpha}$, to the range of macroscopic scales, where the distribution function, in main, is determined by the cutoff factor. We note that for the case when $\xi_{\text{eff}} < 1$, due to the cutoff factor, the contribution of the integration over the region beyond the effective cutoff parameter ξ_{eff} in the value integral (4) is small in comparison with the contribution from the integration over the region $[\mu, \xi_{\text{eff}}]$. Several simple asymptotic relationships can be obtained for the macroscopic porosity from Eq. (7) for certain relations between the value of ξ_{eff}, which characterizes the morphology of the medium, and the value of $\xi_{\max}$, which is an upper limit of the measuring interval $[\lambda/\Lambda, 1]$. Let us consider two limiting cases.

(a) Porosity in the case when the morphological interval is significantly broader than the measuring interval.

In this limiting case the effective cutoff length of the morphologic interval is significantly larger than the upper limit of the measuring interval $[\lambda/\Lambda, 1]$, i.e., we have $\xi_{\text{eff}} \gg \xi_{\max} = 1$. For the porous medium comprising a multitude of the connected pores a distribution of the parameter ξ [Eq. (5)] is a distribution of the percolation type.[78] Hence, the situation considered in this limiting case is related to the state above the percolation threshold of the porous space through the macroscopic cell of the linear size Λ. We remind that the macroscopic sells are the elementary statistical units, which were used for organization of the statistical ensemble of the random fractal model.

Further, taking into account that the parameter β in the cutoff factor has a positive value around unity (see Table I), we obtain that $b \ll 1$. Then, by assuming that the measuring interval is broad, i.e., $\mu \ll 1$, we also obtain that $b\mu^{\beta} \ll 1$. By using the power series expansions of the Incomplete Gamma function[79]

$$\Gamma(q,x) = \Gamma(q) - \sum_{n=0}^{\infty} \frac{(-1)^n x^{q+n}}{n(q+n)}, \quad \text{for } x < 1 \tag{8}$$

and keeping only the first nonvanishing terms of the series containing the parameter b in the numerator and denominator of Eq. (7), we obtain

$$\Phi \approx \frac{1+\alpha}{1+\alpha+d-D} \; \frac{1-\mu^{1+\alpha+d-D}}{1-\mu^{1+\alpha}}, \tag{9}$$

Note that this equation was also obtained by Nigmatullin[70] on the basis of the generalized fractal conception, where he considered only a power factor in our general relationship [Eq. (5)] for scale distribution function.

In order to make more tractable relationship for the porosity, further two possibilities for obtaining the asymptotic equations for the macroscopic porosity on the basis of Eq. (9) can be considered.

(i) The first simplification can be obtained when the exponents $1+\alpha+d-D$ and $1+\alpha$ are positive. These two inequalities are fulfilled when $\alpha > -1$ (since $d-D > 0$). In this case, by taking in to account that $\mu \ll 1$, the macroscopic porosity reads as

$$\Phi \approx \frac{1+\alpha}{1+\alpha+d-D}. \tag{10}$$

Then, if the rate of the change of the distribution function in the mesoscale region is small, i.e., $|\alpha| \ll 1$, for Euclidean three dimensional space, $d=3$, we obtain a simple approximate relationship between the average porosity of a glass and the fractal dimension of the pore space, which reads

$$\Phi \approx \frac{1}{4-D}. \tag{11}$$

(ii) The second simplification for the macroscopic porosity from Eq. (9) can be obtained when the exponents $1+\alpha+d-D$ and $1+\alpha$ are negative, which yields the condition $\alpha < -(1+d-D)$. This case corresponds to the situation of the rapid decay of the distribution function $w(\xi)$ according to the power low in the mesoscale region. For this case we have $\mu^{1+\alpha+d-D} \gg 1$. Hence, the macroscopic porosity reads as

$$\Phi \approx \frac{1+\alpha}{1+\alpha+d-D}\, \mu^{d-D}. \tag{12}$$

It is relevant to note here that despite the initial assumption of a scaling distribution function $w(\xi)$, depending on the value of parameter α characterizing the rate of the distribution function decay, the random fractal model in the asymptotic regime yields two qualitatively different results, expressed by Eqs. (11) and (12). One can see that the porosity expressed by Eq. (11) does not obtain the scaling properties, while in the second case, Eq. (12) provides a length scaling regime due to the factor μ^{d-D}.

(b) Porosity in the case when the morphological interval is significantly narrower than the measuring interval.

In this limiting case the following condition is fulfilled: $\xi_{\text{eff}} \ll \xi_{\max} = 1$. This means that the upper boundary of the measuring interval, $\xi_{\max}$ is essentially higher than the cutoff length ξ_{eff} of the mesoscale morphological interval. In contrast to the previous case (a), which was related to the situation above the percolation threshold of the porous space through the macroscopic cell of the linear size Λ, the present limiting case corresponds to the state below the percolation threshold on this scale.[78] Note that this situation corresponds to the case of the pore clusters, which are limited in size, and they do not span the sample.

For the simplification of Eq. (7) we further assume that the range of the scaling regime was broad enough to fulfill the condition that the lower boundary of the measuring interval will be essentially less than ξ_{eff}, i.e., $\mu \ll \xi_{\text{eff}}$. These two conditions yield the following equivalent inequalities: $b \gg 1 \gg b\mu^{\beta}$. Since, the Gamma function $\Gamma(q,x)$ decays faster than exponentially in the limit of large values of the variable x, i.e.,

$$\Gamma(q,x) \sim x^{q-1} \exp(-x)[1 + O(1/x)], \quad \text{for } x \to \infty \tag{13}$$

we can neglect the terms $\Gamma((1+\alpha+d-D)/\beta, b)$ and $\Gamma((1+\alpha)/\beta, b)$ in Eq. (7) for $b \gg 1$. Hence, the macroscopic porosity reads as

$$\Phi = \frac{1}{b^{(d-D)/\beta}} \frac{\Gamma((1+\alpha+d-D)/\beta, b\mu^{\beta})}{\Gamma((1+\alpha)/\beta, b\mu^{\beta})}. \quad (14)$$

Further, by using the condition $b\mu^{\beta} \ll 1$ and the expansions of the Incomplete Gamma function (8), Eq. (14) yields

$$\Phi = \frac{1}{b^{(d-D)/\beta}} \cdot \frac{1+\alpha}{1+\alpha+d-D} \times \frac{\Gamma\left(\frac{1+\alpha+d-D}{\beta}+1\right) - (b\mu^{\beta})^{1+\alpha+d-D}}{\Gamma\left(\frac{1+\alpha}{\beta}+1\right) - (b\mu^{\beta})^{1+\alpha}}, \quad (15)$$

where $\Gamma(q) = \Gamma(q,0) = \int_0^{\infty} x^{q-1} \exp(-x) dx$ is the Gamma function.

For the further simplification of Eq. (15) we follow the same procedure as above and require the exponents $1+\alpha+d-D$ and $1+\alpha$ to be positive. Then the arguments of both Gamma functions in Eq. (15) should be larger than 1. In this case the Gamma functions themselves will be larger than 1 and the following conditions will be fulfilled

$$\frac{(b\mu^{\beta})^{1+\alpha+d-D}}{\Gamma\left(\frac{1+\alpha+d-D}{\beta}+1\right)} \ll 1, \quad (16a)$$

$$\frac{(b\mu^{\beta})^{1+\alpha}}{\Gamma\left(\frac{1+\alpha}{\beta}+1\right)} \ll 1. \quad (16b)$$

Thus for the macroscopic porosity we obtain

$$\Phi = \frac{1}{b^{(d-D)/\beta}} \frac{1+\alpha}{1+\alpha+d-D} \frac{\Gamma\left(\frac{1+\alpha+d-D}{\beta}+1\right)}{\Gamma\left(\frac{1+\alpha}{\beta}+1\right)}. \quad (17)$$

In order to obtain a more tractable relationship for Φ, further simplification may be made if we assume an additional condition $\beta = 1$, which corresponds to the percolation form of the size-distribution function.[78] Then, by using an assumption of a small rate of change of the distribution function in the mesoscale region, i.e., $|\alpha| \ll 1$, for Euclidean three-dimensional space, $d = 3$, we obtain

$$\Phi \approx \frac{\Gamma(5-D)}{b^{3-D}} \frac{1}{4-D}, \quad (18)$$

Note that Eq. (18), corresponding to the present case, when $b \gg 1$, differs from Eq. (11), obtained in the previous limiting case (a), when $b \ll 1$, by the factor $\Gamma(5-D)/b^{3-D}$. This factor may be around or less than 1 for large b depending on D. (c) Scope of utilization of the random fractal model for macroscopic porosity.

The theoretical results of this section are summarized in Table II. As one can see, the random fractal model is capable to describe several different structural organization of porous medium. In order to select from Table II an appropriate equation for the macroscopic porosity one has to know a priori information on the structure of the porous medium. Hence, one of the features of the porous medium is whether the pore clusters are opened or closed on the maximal length scale of the measuring interval. This distinction is characterized by inequalities limiting the value of the parameter b. Thus the case of opened pore clusters corresponds to the state of percolation above the threshold (see numbers 1 through 4 of Table II). On the other hand, the case of closed pore clusters corresponds to the state below the percolation threshold (see numbers 5 through 7 of Table II).

Additionally, one has to know a width of the interval of self similarity of porous space and a width of the measuring interval. In particular, the width of the measuring interval is determined by the parameter μ. Therefore, the cases corresponding to the narrow measuring interval are taken in numbers 1, 5, and 6 of Table II. On the other hand, the cases corresponding to broad measuring interval are taken in numbers 2, 3, 4, and 7.

Parameter $b\mu^{\beta}$ characterizes the relation between the width of the measuring interval and the width of the interval of self similarity of porous space. This relation is characterized by the corresponding inequalities in Table II.

Finally, a value of the rate parameter of the distribution function decay α affects the scaling properties of the macroscopic porosity. Indeed, the scaling property, $\phi(c\mu) = c^{d-D}\phi(\mu)$, of the porosity observed in the regular fractal model [see Eq. (2)], is not fulfilled after statistical averaging [see Eq. (7)]. Therefore, the porosity of porous medium described by the random fractal model built up from superposition of fractal objects having the same fractal dimension, in general, does not demonstrate a scaling behavior. Meanwhile, as was mentioned above, in one special case (see number 4 of Table II) the scaling properties are fulfilled.

B. Determination of the fractal dimension of porous glasses from the dielectric spectroscopy measurements at percolation

The pores in porous silica glass form topologically connected pore channels. Charge carriers such as protons and ions can move along the pore surface. The movement results in a transfer of the electric excitation within the channels along random paths. As was mentioned in the introduction, in order to describe the mechanism of dielectric relaxation associated with this transfer, we follow the ideas developed in Refs. 67 and 68, where a transfer of the excitation of a donor molecule to an acceptor molecule in various condensed media through many parallel channels were considered.

A transfer of the electric excitation along the developed fractal structure of connected pores can be described by the normalized dipole correlation function (DCF) $\Psi(t)$. The correlation function is associated with the relaxation of the entire induced macroscopic fluctuation dipole moment $\overline{M}(t)$ of the sample unit volume, which is equal to the vectorial sum of all the fluctuation dipole moments of pores

$$\Psi(t) \approx \frac{\langle \overline{M}(0) \cdot \overline{M}(t) \rangle}{\langle \overline{M}(0) \cdot \overline{M}(0) \rangle}, \quad (19)$$

where the symbol $\langle\ \rangle$ denotes an ensemble average. The velocity and laws governing the correlation function are di-

TABLE II. The general relationship and the asymptotic equations for the macroscopic porosity at different values of the parameters.

General relationship $$\Phi=\frac{1}{b^{(d-D)/\beta}}\frac{\Gamma\left(\frac{1+\alpha+d-D}{\beta},b\mu^{\beta}\right)-\Gamma\left(\frac{1+\alpha+d-D}{\beta},b\right)}{\Gamma\left(\frac{1+\alpha}{\beta},b\mu^{\beta}\right)-\Gamma\left(\frac{1+\alpha}{\beta},b\right)}$$

(Values of the parameters)					Asymptotic equations Porosity
N	b	$b\mu^{\beta}$	μ	α	Φ
1	$0<b\ll 1$	$0<b\mu^{\beta}\ll 1$	$0<\mu\leqslant 1$	$\lvert a\rvert\geqslant 0$	$\frac{1+\alpha}{1+\alpha+d-D}\,\frac{1-\mu^{1+\alpha+d-D}}{1-\mu^{1+\alpha}}$
2	$0<b\ll 1$	$0<b\mu^{\beta}\ll 1$	$0<\mu\ll 1$	$1+\alpha>0$	$\frac{1+\alpha}{1+\alpha+d-D}$
3	$0<b\ll 1$	$0<b\mu^{\beta}\ll 1$	$0<\mu\ll 1$	$1+\alpha>0$ $\lvert a\rvert\ll 1$	$\frac{1}{4-D}$
4	$0<b\ll 1$	$0<b\mu^{\beta}\ll 1$	$0<\mu\ll 1$	$1+\alpha<d-D$	$\frac{1+\alpha}{1+\alpha+d-D}\,\mu^{d-D}$
5	$b\gg 1$	$b\mu^{\beta}>0$	$0<\mu\leqslant 1$	$\lvert a\rvert\geqslant 0$	$\frac{1}{b^{(d-D)/\beta}}\frac{\Gamma\left(\frac{1+\alpha+d-D}{\beta},b\mu^{\beta}\right)}{\Gamma\left(\frac{1+\alpha}{\beta},b\mu^{\beta}\right)}$
6	$b\gg 1$	$0<b\mu^{\beta}\ll 1$	$0<\mu\leqslant 1$	$\lvert a\rvert\geqslant 0$	$\frac{1}{b^{(d-D)/\beta}}\frac{1+\alpha}{1+\alpha+d-D}\frac{\Gamma\left(\frac{1+\alpha+d-D}{\beta}+1\right)}{\Gamma\left(\frac{1+\alpha}{\beta}+1\right)}$
7	$b\gg 1$	$0<b\mu^{\beta}\ll 1$	$0<\mu\ll 1$	$\lvert\alpha\rvert\ll 1$ $d=3$	$\frac{\Gamma(5-D)}{b^{3-D}}\,\frac{1}{4-D}$

rectly related to the structural and kinetic properties of the sample and characterize the macroscopic properties of the system studied. We note that a transfer of the electric excitation through the porous medium can occur even in the case of closed pores, which are topologically not connected one to another.[80] However, the distance between neighboring closed pores in a glass filled with dielectric or conductive material should be small enough in order to provide a physical coupling between the neighboring pores separated by thin walls via the electric interaction. Note that he physical coupling in the closed pores, for example, can be due to multipolar interactions.[80]

A detailed description of the relaxation mechanism associated with an excitation transfer based on a regular fractal model was introduced earlier,[81] where it was applied for the cooperative relaxation of ionic microemulsions at percolation.

According to this model, an elementary act of the excitation transfer along the length L_j is described by the microscopic relaxation function $g(z/z_j)$, where L_j is the ''effective'' length of a channel of the relaxation in the jth stage of self-similarity. In this function, z_j is a dimensional variable characterizing the jth stage of the self similarity of the fractal system considered, z is the dimensionless time, $z=t/\tau$, where the parameter τ is the minimal relaxation time needed for an excitation to hop from one excitation center to its nearest neighbor.

The following assumption is invoked: $z_j=aL_j$, where a is a coefficient of proportionality. For each stage of the self-similarity j, the time of relaxation $\tau_j=\tau z_j$ is proportional to the length L_j. From fractal geometry,[74,82] L_j can be expressed as

$$L_j=lk^j, \tag{20}$$

where l is the minimal scale and k is a scaling factor ($k>1$). We assume that the total number of activation centers located along the segment L_j also obeys the scaling law

$$n_j=n_0p^j, \tag{21}$$

where p is the scaling factor ($p>1$), and n_0 is the number of the nearest neighbors near the selected center (i.e., $j=0$).

The macroscopic correlation function can be expressed as a product of the relaxation functions $g(z/z_j)$ for all the stages of the self-similarity of the fractal system considered

$$\Psi(z)=\prod_{j=0}^{N}[g(z/z_j)]^{n_j}=\prod_{j=0}^{N}[g(Z\xi^j)]^{n_0p^j}, \tag{22}$$

where $Z=t/al\tau$; $\xi=1/k$ and $N=1/\ln k\ln(L_N/l)$. Here, L_N is the finite geometrical size of the fractal cluster, where N refers to the last stage of the self similarity.

The estimations of the product (22) for various values of $\xi<1$ and $p>1$ are given in Ref. 81. The results of the cal-

culations may be written in the form of a modified Kohlrausch-Williams-Wats (KWW) stretched-exponential relaxation law:

$$\Psi(Z)/\Psi(0)=\exp[-\Gamma(\nu)Z^{\nu}+B(\nu)Z], \tag{23}$$

where the parameters $\Gamma(\nu)$ and $B(\nu)$ are given by

$$\Gamma(\nu)=\frac{n_0}{\ln(1/\xi)}\int_0^{\infty} y^{-\nu}\left|\frac{g'(y)}{g(y)}\right|dy, \tag{24}$$

$$B(\nu)=\frac{n_0 a_1}{\ln(1/\xi)(1-\nu)}\varepsilon^{1-\nu}, \tag{25}$$

where

$$\nu=\ln p/\ln(1/\xi), \tag{26}$$

with $0<\nu<1$, and for $\varepsilon=\xi^N\ll 1$. We note that the parameter Γ depends on the relaxation function g and affects the macroscopic relaxation time $\tau_M=\tau a l\Gamma^{-1/\nu}$, and B is a correction parameter for the KWW function at large times.

The temporal boundaries $\tau_{\min}$ and $\tau_{\max}$ of the applicability of Eq. (23) for describing the cooperative relaxation are determined by the expression:

$$\left|\frac{A_1 n_0}{\overline{g}}\left[\frac{1}{2}-\frac{1}{\ln(1/\xi)(1+\nu)}\right]\right| \ll\frac{t}{a l\tau}\ll\left|\left[\frac{2\ln(1/\xi)(2-\nu)}{n_0(2a_2-a_1^2)\varepsilon^{2-\nu}}\right]^{1/2}\right|. \tag{27}$$

The parameters $\overline{g}$, A_1, a_1, and a_2 in Eqs. (24)–(27) are related to the asymptotic properties of the elementary relaxation function $g(y)$

$$g(y)=1-a_1 y+a_2 y^2+\cdots \quad \text{for } y\ll 1 \tag{28}$$

$$g(y)=\overline{g}+A_1/y+A_2/y^2+\cdots \quad \text{for } y\gg 1. \tag{29}$$

The relationship between the exponent ν, $\nu=\ln p/\ln k$, and the fractal dimension D_p of the paths of excitation transfer may be derived from the proportionality and scaling relations by using an assumption that the fractal is isotropic and has spherical symmetry. The number of pores that are located along a segment of length L_j on the jth step of the self-similarity is $n_j\sim p^j$. The total number of pores in the cluster is $S\sim n_j^d\sim(p^j)^d$, where d is Euclidean dimension, $(d=3)$. The similarity index η, which determines by how much the linear size of the fractal is enlarged at step j, is $\eta\sim L_j\sim k^j$. In this case, we obtain the simple relationship between ν and the fractal dimension D_p as

$$D_p=\ln S/\ln\eta=3j\ln p/j\ln k=3\nu. \tag{30}$$

Further we will focus our attention only on the time dependence behavior of the dipole correlation function $\Psi(t)$ defined by Eq. (23), that is given by

$$\Psi(t)\approx C(t)\exp[-(t/\tau)^{\nu}], \tag{31}$$

where $C(t)$ is the slow growing function of time. By taking into account Eq. (30) and ignoring the slow variation with time of $C(t)$, we obtain the asymptotic stretched-exponential term

$$\Psi(t)\sim\exp[-(t/\tau)^{D_p/3}], \tag{32}$$

that can be further fitted to the experimental correlation functions in order to determine the value of the fractal dimension of the paths of excitation transfer within the porous medium. If the fractal dimension of these paths coincides with the fractal dimension of the pore space, then it can be used in the asymptotic equations derived above for obtaining the porosity.

III. EXPERIMENT

A. Sample preparation

Four silica porous glasses labeled 1, 2, 3, and 4 were fabricated by the leaching of sodium borosilicate glasses with phase separation in acid solutions according to the technology described elsewhere.[83,84] Porosity of samples 1 to 4 was determined by the relative mass decrement method. Additionally, for control, the porosity for sample 4 were calculated by Brunauer-Emmett-Teller (BET) analysis according to the methodology.[40] It is known from the technology of sample fabrication, that sample 1 contains silica gel in the pore's volume, albeit the silica gel is barely present in any the other samples. The dimensions of pores were calculated from absorption-desorption isotherms and from an optical microscope photograph of the porous glass samples.[85] The magnitudes of pore sizes obtained from these two methods concur. However, if the pores are filled up with silica gel, then neither of these methods is accurate for determining the pore sizes. The water content in pores ρ, defined as the ratio of the mass of adsorbed water to the mass of the dry sample, was determined by weighing the samples prior to and after the dielectric measurements. The dimensions of the pores, porosity, and humidity of the samples are presented in Table III.

B. Experimental technique

Dielectric measurements in the frequency range of 20 Hz–1 MHz were performed on samples 1, 2, and 3 by using a Broad Band Dielectric Spectrometer BDS 4284 (NOVOCONTROL) with automatic temperature control by QUATRO Cryosystem. The measurement on sample 4 was performed by a BDS 4000 device in the frequency range of 10^{-2} Hz–3 MHz. The accuracy of the complex dielectric permittivity measured, $\varepsilon^*(\omega)=\varepsilon'(\omega)-i\varepsilon''(\omega)$ [where $\varepsilon'(\omega)$ and $\varepsilon''(\omega)$ are the real and loss parts of the complex permittivity, respectively], was estimated to be better than 3%.[86] The measurements were carried out by cooling the samples from 20 °C down to −100 °C. The samples were then measured at intervals of 5 °C upon heating them from −100 to 300 °C. The size and thickness of the square plate samples, used for dielectric measurements, were 30 and 0.31–0.32 mm, respectively.

TABLE III. Structural parameters obtained from (A) adsorption-desorption isotherms method and from optical microscope photograph, (B) relative mass decrement method, (C) BET analysis, and (D) dielectric spectroscopsy analysis.

Sample \ Method	Dimension of the pores (nm) A	Porosity $\Phi(\%)$ B	Porosity $\Phi(\%)$ C	Humidity $\rho(\%)$ B	Fractal Dimension D_p D	Porosity $\Phi(\%)$ D
1	50÷70	38±1		1.19±0.05	0.99±0.06	33±1
2	50÷70	48±1		1.21±0.05	1.89±0.06	47±1
3	280÷400	38±1		3.20±0.05	1.38±0.06	38±1
4	10÷30	59±1	59±1	1.4±0.05	2.47±0.06	65±1

IV. RESULTS AND DISCUSSION

A. Determination of the fractal dimensions

A typical spectrum of the dielectric permittivity $\varepsilon'(\omega,T)$ of the studied porous glasses versus frequency ω and temperature T is displayed in Fig. 3. For this figure as well as in Fig. 1, we chose sample 2 as an example for the typical illustrations of the dielectric spectroscopy data. The peak of the permittivity at the temperature interval 50–80 °C corresponds to the temperature-driven percolation process associated with the transfer of the electric excitation within the developed structure of connected pores. We note that the characteristic peak corresponding to this percolation process was also indicated on the three-dimensional plot (see Fig. 1) for dielectric losses $\varepsilon''(\omega,T)$.

We shall analyze the dielectric relaxation of the glasses in the time domain since the theoretical relaxation model described above is formulated for the dipole correlation function $\Psi(t)$. By analyzing this dependence at percolation and using Eq. (32), we can determine the fractal dimension of the paths of the excitation transfer D_p.

The complex dielectric permittivity can be expressed in terms of the DCF as follows:

$$\varepsilon^*(\omega)=\varepsilon_\infty-(\varepsilon_s-\varepsilon_\infty)\hat{F}\left(\frac{d}{dt}\Psi(t)\right), \tag{33}$$

where $\hat{F}$ is the operator of the Fourier transform, and the parameters ε_s and ε_∞ are the static dielectric permittivity and its high-frequency limit, respectively. Figure 4 shows a typical example of the DCF, corresponding to sample 2, obtained from the frequency dependence of the complex permittivity at the percolation temperature. One can see that the DCF displays a complex nonexponential time behavior that can be deconvoluted into the sum of two processes with the characteristic relaxation times of around 10^{-5} and 10^{-2} seconds. The short relaxation time is related to that relaxation process which has a saddlelike shape in Fig. 1, while the long time process in Fig. 4 is associated with the percolation process. This long time behavior of the DCF can be fitted to Eq. (32) with the purpose of determining the fractal dimension D_p. The resulting values of D_p are presented in Table III.

One can see that the fractal dimension of the excitation paths in sample 1 is close to unity. Topologically, this value of D_p corresponds to the propagation of the excitation along a linear path that may correspond to a presence of silica gel within the pores. Indeed, the silica gel creates a subsidiary tiny scale matrix with an enlarged number of hydration centers within the pores. Since these centers are distributed in the pore volume, the excitation transmits through the volume and is not related to the hydration centers located on the pore surface of the connective pores. Due to the large number of the hydration centers, and the short distance between the

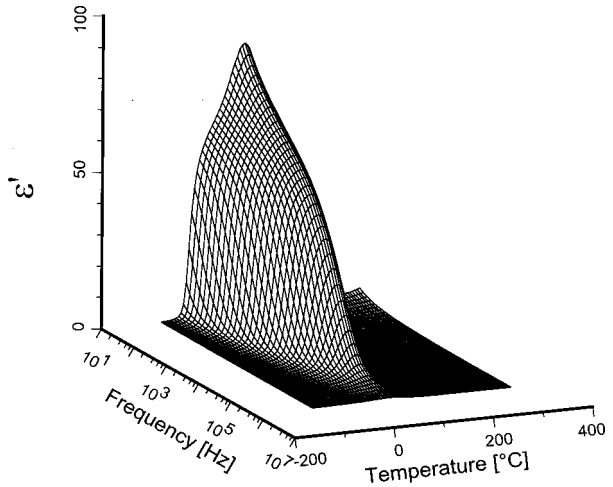

FIG. 3. Three-dimensional plot of the frequency and temperature dependence of the dielectric permittivity of sample 2.

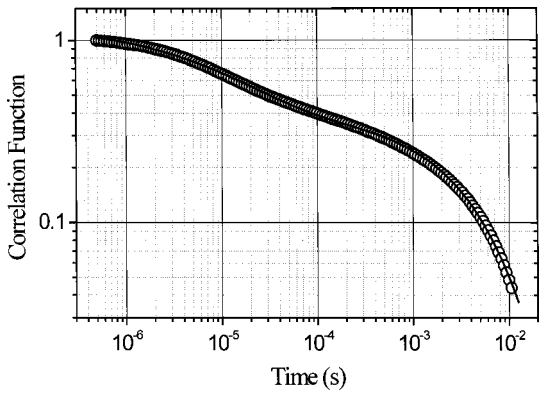

FIG. 4. Log-log plot of the macroscopic correlation function of sample 2 at the temperature corresponding to percolation. The solid line corresponds to a fit of the sum of two KWW relaxation functions.

neighboring centers, the path can be approximated by a line with a fractal dimension around unity.

The fractal dimensions of the excitation paths in samples 2 and sample 3 have values between 1 and 2. In contrast to sample 1, the silica gel in these samples is leached out, i.e., water molecules are adsorbed on the inner pore surface. Therefore, despite the fact that according to the literature the fractal dimension of a rough pore surface should be around 2.5 with the upper-length cutoff <20 Å (Ref. 35), the small values of D_p observed in samples 2 and 3 can be explained by one of two ways. On the one hand, the surface can be defractalized upon deposition of an adsorbed film of water, which results in the ''smoothing'' of the surface. On the other hand, the transfer of the excitation in these samples occurs along the inner-pore surface from one hydration center to another. The distance between the centers can be significantly larger than the small-scale details of the surface texture. Therefore, the fractal dimension observed is that of the chords connecting the hydration centers, which should be lesser than 2. An investigation of the problem of which way of these two is more appropriate for the systems studied is beyond the scope of the current paper, and it will be discussed in our further work.

The fractal dimensions of the excitation paths in sample 4 is greater than 2. In order to explain this magnitude we note that the characteristic size of pores in this sample is significantly smaller than that in samples 1–3 (see Table III). Therefore, the distance between the neighboring hydrated centers located on the surface can be comparable with the pore size. Thus we can expect that the transfer occurs across the pore bulk from the one pore wall to another wall rather than along the pore surface.

In concluding this section it is relevant to note that the fractal dimensions discussed here are the fractal dimensions of the excitation transfer paths connecting the hydration centers located on the inner surface of the pores. The magnitudes of fractal dimensions obtained for samples 2 and 3 is less than 2, which is in agreement with the data obtained from the energy-transform measurements.[21,38] Due to the small value of humidity ρ, all the water molecules absorbed by the materials are bound to these centers. The paths of the excitation transfer span along the fractal pore surface and ''depict'' the backbone of clusters formed by the pores on a scale that is larger than the characteristic distance between the hydration centers on the pore surface. Thus the fractal dimension of the paths is an approximation of the real surface fractality and it can be used for porosity calculations in this scale interval.

B. Determination of porosity

For a calculation of the macroscopic porosity of a porous medium, the general Eq. (7) can be used. In such a general case, this is a difficult task due to the large number of parameters, such as D, α, β, μ, and b, which must be known. However, when the system in the measured scale interval has certain morphological features, the more simplified asymptotic relationships obtained in Sec. II [Eqs. (9)–(12), and Eqs. (14)–(18)] can be used.

We note that a well-developed porous structure of open connective pores is obtained as a result of the leaching out of the acid-soluble phase from sodium borosilicate glasses. This ramified pore space can be considered as a system of random percolating pore clusters. Hence, polydispersity of the clusters can be described by the general distribution functions, Eq. (5), with the parameters corresponding to the distribution of the percolation type.[78]

One has to bear in mind that the theoretical values of the percolation threshold of the bond and site percolation models are 0.25 and 0.31, respectively.[87] The porosity of the silica porous glasses obtained on the basis of the relative mass decrement method (see Table III) is larger than these theoretical values of the percolation threshold. Therefore, we assume that the glasses investigated are beyond the percolation threshold. In this case $\xi_{\text{eff}} \rightarrow \infty$, and the main condition, $b \ll 1$, for the application of Eq. (9) is fulfilled. Further, we note that since the experimental time range of the dielectric measurements is wide, the corresponding interval of space scales is also wide, i.e. the condition $\mu = \lambda/\Lambda \ll 1$ is fulfilled. The fulfillment of that condition may allow us to use Eq. (10) for the determination of the porosity. A final simplification can be made after taking into account that the scaling interval in the well-developed system of pore clusters is wide. This allows us to assume that the distribution function decreases slowly within the measuring interval, i.e., $|\alpha| \ll 1$. The assumptions considered allows us to choose a simple one-parametric Eq. (11) from the set of the various asymptotic equations, which establishes the relationship between the fractal dimension of the porous space and the macroscopic porosity of the material. The results of the porosity calculation using Eq. (11) and the fractal dimension determined from dielectric measurements are shown in the last column of Table III. These values can be compared with the porosity determined from the relative mass decrement measurements shown in the same table. As one can see, the values obtained from dielectric spectroscopy concur well with the porosity data obtained from the relative mass decrement method.

V. SUMMARY

The dielectric relaxation process associated with percolation of the electric excitation within the developed fractal structure of connected pores was analyzed in order to determine the porous morphology in silica glasses. For this purpose, we developed a statistical model of porous media based on ideas of fractal geometry, establishing a relationship between the fractal dimension and the value of macroscopic porosity of the material. Several simple asymptotic relationships have been obtained in the framework of the model for a quantitative characterization of the porosity. An application of these relationships for calculation of porosity depends on certain relations between the value of the cutoff length of the size polydispersity distribution function, which characterizes the morphology of the medium, and the value of the upper limit of the measuring length scale interval. The model developed has been applied in the investigation of porous silica glasses. A determination of the characteristic intervals of variations of the model parameters corresponding to the morphology of connected pores enabled us to select the appropriate asymptotic equation for the macroscopic porosity [Eq. (11)]. In this simple equation, the porosity is determined by one parameter, which is the fractal dimension

of the porous space. The fractal dimension determined for the paths along which the transfer of the electric excitation occurs in the developed morphology of the connected pore channels was used to estimate the porosity. This value of the fractal dimension was obtained from the experimental dielectric data on the basis of the dynamic theory of the cooperative relaxation process describing the percolation within the porous medium.

The fractal dimensions obtained for the studied porous silica glasses vary over in the broad interval between 1 and 2.5. If the amount of the adsorbed water is small, then all the water molecules are bound to the hydration centers and located on the inner surface of the pores. The excitation transfers through the medium depict a path connecting the centers. The values obtained from dielectric spectroscopy do not contradict the literature data mentioned in the introduction and are also in good agreement with the values obtained from the energy-transform measurements. The concurrence of the macroscopic porosity values obtained from dielectric spectroscopy method developed in this paper and the values obtained from the relative mass decrements method are results of the accurate determination of the fractal dimensions and the validity of the statistical model of the macroscopic porosity used here.

ACKNOWLEDGMENTS

We would like to express our appreciation to Raoul Nigmatullin for inspiration in writing this paper and helpful discussions. A. G. acknowledges the support of the Israel Ministry of Science and Technology.

*Author to whom correspondence should be addressed. FAX: +972 2 5663878. Electronic address: yurif@vms.huji.ac.il

[1] M. H. Reich, S. P. Russo, I. K. Snook, and H. K. Wagenfeld, J. Colloid Interface Sci. **135**, 353 (1990).
[2] W. I. Friesen and R. J. Micula, J. Colloid Interface Sci. **120**, 263 (1987).
[3] E. D. Safronsky, Ya. O. Roizin, and E. Rysiakiewicz-Pasek, Opt. Mater. **5**, 217 (1996).
[4] Paul W. Schmidt, in *The Fractal Approach to Heterogeneous Chemistry: Surfaces, Colloids, Polymers*, edited by D. Avnir (Wiley, New York, 1989), p. 67.
[5] D. W. Schaefer and K. D. Keefer, Phys. Rev. Lett. **56**, 2199 (1986).
[6] J. C. Li, D. K. Ross, L. D. Howe, K. L. Stefanopoulos, J. P. A. Fairclough, R. Heenan, and K. Ibel, Phys. Rev. B **49**, 5911 (1994).
[7] Po-zen Wong, J. Howard, and Jar-Shyong Lin, Phys. Rev. Lett. **57**, 637 (1986).
[8] D. W. Schaefer and K. D. Keefer, Phys. Rev. Lett. **53**, 1383 (1984).
[9] P. R. Johnston, P. McManon, M. H. Reich, I. K. Snook, and H. K. Wagenfeld, J. Colloid Interface Sci. **155**, 146 (1993).
[10] H. D. Bale and P. W. Schmidt, Phys. Rev. Lett. **53**, 596 (1984).
[11] D. F. R. Mildner and P. L. Hall, J. Phys. D **19**, 1535 (1986).
[12] M. J. Benham, J. C. Cook, J-C. Li, D. K. Ross, P. L. Hall, and B. Sarkissian, Phys. Rev. B **39**, 633 (1989).
[13] F. Katsaros, P. Makri, A. Mitropoulos, N. Kanellopoulos, U. Keiderling, and A. Wiedenmann, Physica B **234–236**, 402 (1997).
[14] A. Höhr, H.-B. Neumann, P. W. Schmidt, P. Pfeifer, and D. Avnir, Phys. Rev. B **38**, 1462 (1988).
[15] SH. Chen and S. Choi, Supramol. Sci. **5**, 197 (1998).
[16] D. Cazorla-Amoros, CSM. de Lecea, J. Alcaniz-Monge, M. Gardner, A. Noth, and J. Dore, Carbon **36**, 309 (1998).
[17] A. J. Katz and A. H. Thompson, Phys. Rev. Lett. **54**, 1325 (1985).
[18] C. E. Krohn and A. H. Thompson, Phys. Rev. B **33**, 6366 (1986).
[19] P. Evesque, in *The Fractal Approach to Heterogeneous Chemistry: Surfaces, Colloids, Polymers*, edited by D. Avnir (Wiley, New York, 1989), p. 81.
[20] P. Levitz, G. Ehret, S. K. Sinha, and J. M. Drake, J. Chem. Phys. **95**, 6151 (1991).
[21] U. Even, K. Rademann, J. Jortner, N. Manor, and R. Reisfeld, Phys. Rev. Lett. **52**, 2164 (1984).
[22] D. Pines and D. Huppert, Chem. Phys. Lett. **156**, 223 (1989).
[23] C. L. Yang, P. Evesque, and M. A. El-Sayed, J. Phys. Chem. **89**, 3442 (1985).
[24] J. J. Fripiat, in *The Fractal Approach to Heterogeneous Chemistry: Surfaces, Colloids, Polymers*, edited by D. Avnir (Wiley, New York, 1989), p. 331.
[25] J. M. Drake, L. N. Yacullo, P. Levitz, and J. Klafter, J. Phys. Chem. **98**, 380 (1994).
[26] P. Pfeifer and D. Avnir, J. Chem. Phys. **79**, 3558 (1983).
[27] D. Avnir, D. Farin, and P. Pfeifer, J. Chem. Phys. **79**, 3566 (1983).
[28] M. Jaroniec, X. Lu, R. Maday, and D. Avnir, J. Chem. Phys. **92**, 7589 (1990).
[29] M. Sato, T. Sukegawa, T. Suzuki, and K. Kaneko, J. Phys. Chem. B **101**, 1845 (1997).
[30] J-C. Li and D. K. Ross, J. Phys.: Condens. Matter **6**, 351 (1994).
[31] A. Ch. Mitropoulos, P. K. Makri, N. K. Kanellopoilos, U. Keiderling, and A. Wiedenmann, J. Colloid Interface Sci. **193**, 137 (1997).
[32] D. F. R. Mildner and P. L. Hall, J. Phys. D **19**, 1535 (1986).
[33] S. Ozeki, Langmuir **5**, 186 (1989).
[34] H. D. Bale and P. W. Schmidt, Phys. Rev. Lett. **53**, 596 (1984).
[35] M. Agamalian, J. M. Drake, S. K. Sinha, and J. D. Axe, Phys. Rev. E **55**, 3021 (1997).
[36] P. Wiltzius, F. S. Bates, S. B. Dierker, and G. D. Wignall, Phys. Rev. A **36**, 2991 (1987).
[37] A. Ch. Mitropoulos, J. M. Haynes, R. M. Richardson, and N. K. Kanellopoulos, Phys. Rev. B **52**, 10 035 (1995).
[38] U. Even, K. Rademann, J. Jortner, N. Manor, and R. Reisfeld, Phys. Rev. Lett. **58**, 285 (1987).
[39] P. M. Adler, in *The Fractal Approach to Heterogeneous Chemistry: Surfaces, Colloids, Polymers*, edited by D. Avnir (Wiley, New York, 1989), p. 341.
[40] S. J. Gregg and K. S. W. Sing, *Adsorption, Surface Area and Porosity* (Academic, New York, 1982).
[41] F. Rodrguez-Reinoso, *Characterization of Porous Solids* (Elsevier, New York, 1991).
[42] Y. Guo, K. H. Langley, and F. E. Karasz, Phys. Rev. B **50**, 3400 (1994).
[43] J. de Kinder, A. Bouwen, and D. Schoemaker, Phys. Lett. A **203**, 251 (1995).
[44] J. de Kinder, A. Bouwen, and D. Schoemaker, Phys. Rev. B **52**, 15 872 (1995).

[45] P. E. Sokol, R. T. Azuah, M. R. Gibbs, and S. M. Bennington, J. Low Temp. Phys. **103**, 23 (1996).
[46] S. Peleg, J. Naor, R. Hartley, and D. Avnir, IEEE Trans. Pattern. Anal. Mach. Intell. **PAMI-6**, 518 (1984).
[47] H. Takayasu, *Fractals in the Physical Sciences* (Manchester University Press, Manchester, 1990).
[48] R. Hilfer, Adv. Chem. Phys. **XCII**, 299 (1996).
[49] W. D. Dozier, J. M. Drake, and J. Klafter, Phys. Rev. Lett. **56**, 197 (1986).
[50] F. Grinberg and R. Kimmich, J. Chem. Phys. **105**, 3301 (1996).
[51] T. Zavada, S. Stapf, U. Beginn, and R. Kimmich, Magn. Reson. Imaging **16**, 711 (1998).
[52] S. Stapf, R. Kimmich, RO. Seitter, A. I. Maklakov, and V. D. Skirda, Colloids Surf., A **115**, 107 (1996).
[53] R. Hilfer and W. E. Kenyon, J. Appl. Phys. **55**, 3153 (1983).
[54] I. Holwech and B. Nøst, Phys. Rev. B **39**, 12 845 (1989).
[55] B. Nettelblad and G. A. Niklasson, J. Phys.: Condens. Matter **8**, 2781 (1996).
[56] B. Nettelblad and G. A. Niklasson, J. Mater. Sci. **32**, 3783 (1997).
[57] J. P. Calame, A. Birman, Y. Carmel, D. Gershon, B. Levush, A. A. Sorokin, V. E. Semenov, D. Dadon, L. P. Martin, and M. Rosen, J. Appl. Phys. **80**, 3992 (1996).
[58] L. C. Shen, C. Liu, J. Korringa, and K. J. Dunn, J. Appl. Phys. **67**, 7071 (1990).
[59] T. J. Heimovaara, W. Bouten, and J. M. Verstraten, Water Resour. Res. **30**, 201 (1994).
[60] Shmulik P. Friedman, Soil Sci. Soc. Am. J. **61**, 742 (1997).
[61] R. Hilfer, Phys. Rev. B **44**, 60 (1991).
[62] R. Hilfer, Phys. Scr. **T44**, 51 (1992).
[63] J. B. Hasted, *Aqueous Dielectrics* (Chapman and Hall, London, 1973).
[64] A. Gutina, E. Axelrod, A. Puzenko, E. Rysiakiewicz-Pasek, N. Kozlovich, and Yu. Feldman, J. Non-Cryst. Solids **235–237**, 302 (1998).
[65] P. Pissis, J. Laudat, D. Daoukaki, and A. Kyritsis, J. Non-Cryst. Solids **171**, 201 (1994).
[66] M. Nogami and Y. Abe, Phys. Rev. B **55**, 12 108 (1997).
[67] J. Klafter and A. Blumen, Chem. Phys. Lett. **119**, 377 (1985).
[68] J. Klafter and M. F. Shlesinger, Proc. Natl. Acad. Sci. USA **83**, 848 (1986).
[69] A. Doi, J. Mater. Sci. **22**, 761 (1987).
[70] R. R. Nigmatullin, Phys. Status Solidi B **133**, 713 (1986).
[71] *The Fractal Approach to Heterogeneous Chemistry: Surfaces, Colloids, Polymers*, edited by D. Avnir (Wiley, New York, 1989).
[72] D. Gimenez, E. Perfect, W. J. Rawls, and Ya. Pachepsky, Eng. Geology **48**, 161 (1997).
[73] B. B. Mandelbrot, in *The Fractal Approach to Heterogeneous Chemistry: Surfaces, Colloids, Polymers*, edited by D. Avnir (Wiley, New York, 1989), p. 45.
[74] B. B. Mandelbrot, *The Fractal Geometry of Nature* (Freeman, New York, 1982).
[75] P. J. Flory, *Principles of Polymer Chemistry* (Cornell, Ithaca, New York, 1953).
[76] A.-Q. Tang, *Statistical Theory of Plymer Reactions* (Academic, Beijing, 1985).
[77] L. H. Peebles, Jr., *Molecular Weight Distributions in Polymers* (Wiley-Interscience, New York, 1971).
[78] D. Stauffer and A. Aharony, *Introduction to Percolation Theory* (Taylor & Francis, London, 1994), p. 8.
[79] *Handbook of Mathematical Functions with Formulas, Graphs, and Mathematical Tables*, edited by Milton Abramowitz and Irene A. Stegun (Dover, New York, 1972).
[80] F. Claro and F. Brouers, Phys. Rev. B **40**, 3261 (1989).
[81] Yu. Feldman, N. Kozlovich, Y. Alexandrov, R. Nigmatullin, and Y. Ryabov, Phys. Rev. E **54**, 5420 (1996).
[82] E. Feder, *Fractals* (Plenum, New York, 1988).
[83] E. Rysiakiewicz-Pasek and K. Marczuk, J. Porous Mater. **3**, 17 (1996).
[84] Ya. O. Roizin, A. Alexeev-Porov, S. A. Gevelyuk, D. P. Savin, E. Mugenski, I. Sokolska, E. Rysiakiewicz-Pasek, and K. Marczuk, Phys. Chem. Glasses **37**, 196 (1996).
[85] A. V. Alexeev-Porov, Ya. O. Roizin, E. Rysiakiewicz-Pasek, and K. Marczuk, Opt. Mater. **2**, 249 (1993).
[86] G. Schaumburg, Dielectrics Newsletter **2**, 5 (1997).
[87] J. P. Clerc, G. Giraud, J. Laugier, and J. Luck, Adv. Phys. **39**, 191 (1990).